

## **Atlanta Fiber System Experiment:**

# **GaAlAs Laser Transmitter for Lightwave Transmission Systems**

By P. W. SHUMATE, JR., F. S. CHEN, and P. W. DORMAN

(Manuscript received February 16, 1977)

*A feedback-stabilized GaAlAs injection laser optical-communication source for transmission of NRZ data at 44.736 Mb/s has been built and tested. The emitter-coupled driver circuit and the feedback scheme utilizing an operational amplifier are described. Two special hybrid packages contain the circuit components on thick-film substrates, and the package holding the laser provides laser heat-sinking as well as the interface between the laser and optical fiber. The laser source packages that were fabricated were capable of launching an average power of  $>0.5$  mW into the  $55\text{-}\mu\text{m}$  diameter core of a graded-index fiber ( $N.A. = 0.23$ ). The sources draw a total of  $0.9$  W from the  $+5.0$  V and  $-5.2$  V ( $\pm 5$  percent) supplies and operate properly over a temperature range of  $5^\circ$  to  $55^\circ\text{C}$ .*

## **I. INTRODUCTION**

An experimental lightwave communication system has been designed and set up in an environment approaching field conditions at the Bell Laboratories facility in Norcross, Georgia to study the feasibility of optical fiber transmission systems in interoffice digital trunking.<sup>1</sup> The experimental system operates at the DS-3 signal rate (44.736 Mb/s, the third level of the Bell System digital hierarchy) using a binary (on-off) nonreturn-to-zero (NRZ) signal format. Terminal transmitters and line regenerators require an optical source to convert the ECL-level logic signals to optical signals of 0.5 mW average power into a transmission fiber. GaAlAs injection lasers are sources well suited for this application, as they can be on-off modulated at high speeds (with rise times of less than 1 ns) with low drive power. In addition, the laser light can be effi-

ciently coupled into low N.A. fibers, and the laser wavelength and linewidth are nearly optimum for digital transmission in low-loss glass fibers. However, some inherent disadvantages must be circumvented before GaAlAs lasers can be used in practical optical fiber systems, the most important of which is the temperature sensitivity of the laser.

A two-package GaAlAs laser source subsystem was designed and built to operate at 44.7 Mb/s over the temperature range 5° to 55°C. One package contains the GaAlAs double-heterostructure injection laser operating at 825 nm and the driver modulation circuitry. This package also interfaces the laser to the fiber. The second package contains circuitry to provide closed-loop feedback control of the laser output power, rendering this insensitive to changes in ambient temperature or changes in laser parameters due to aging. Sixty-two functioning subsystems were fabricated. This paper describes the circuits and packages and gives data on the overall source subsystem performance as a function of temperature including output power, power stability, pulse response, extinction ratio, and amplitude ripple.

## II. DRIVER CIRCUIT

For the 44.736-Mb/s trunking application, the following requirements were specified. First, the peak light-pulse output must remain constant, regardless of changes in temperature or changes due to laser aging. Second, the extinction ratio (on-off ratio of the light pulses) should be  $\geq 10$  to avoid an excessive sensitivity penalty at the receiver.<sup>2</sup> Third, the delay time between the application of a current pulse and the onset of laser emission must be much shorter than the bit interval so that the light pulses accurately reproduce the digital input signal. Fourth, the relaxation oscillation of the light-output pulses excited by the application of fast current pulses should be damped. Depending on the design of the system, this oscillation may degrade the system's performance. The driver circuit described in this section, used with the laser bias circuit described in the next section, meets these four requirements for a 44.7-Mb/s source subsystem.

Figure 1 shows the response of a semiconductor laser diode to current through the device. A typical diode exhibits spontaneous or LED light for currents below about 100 mA, the lasing threshold. Above this threshold, the output is predominantly coherent laser light. The ratio between these two levels determines the on and off states in the digital signal. To operate at  $>10:1$  on-to-off ratio in the laser transmitter, the diode is biased slightly below threshold at  $I_B$  ( $\sim 90$  mA) in the off or zero state. A high-speed driver then adds an additional current  $I_D$  ( $\sim 20$  mA) for a one state to bring the light level up to the on level. This scheme results in efficient, high-speed operation because the diode capacitance need not be charged repeatedly and the turn-on delay time of the laser

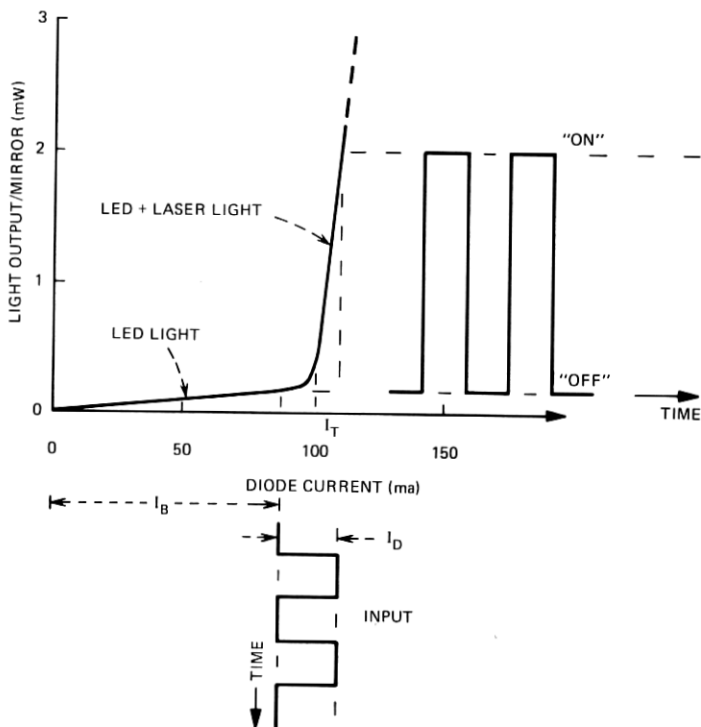


Fig. 1—Transfer characteristic of a semiconductor laser, shown with input (current) waveform and resulting light output.

emission is minimized. The demands placed on the high-speed switch are reduced since  $I_D \ll (I_B + I_D)$ . Undesirable effects due to pattern-dependent junction heating are minimized since the on and off power dissipations are nearly equal. Finally, the principal benefit of this biasing scheme is that the dc bias can be varied easily in a low-frequency, closed-loop manner to stabilize the light output of the laser. This can correct for slow changes in ambient temperature or gradual aging of the laser itself.

The drive current  $I_D$  is provided by an emitter-coupled current switch which supplies constant-amplitude pulses directly to the laser terminal. During assembly, these pulses, with switching speeds of approximately 2 ns, are adjusted in amplitude to match the particular laser being used and left unchanged as the laser ages. This driver circuit is shown in Fig. 2. Transistors  $Q_1$  and  $Q_2$ , forming the current switch, are a conventional emitter-coupled pair. When the base of  $Q_1$  is more positive than the base of  $Q_2$ , all the current ( $= I_D$ ) from the current source is steered through the collector of  $Q_1$  and no drive current passes through the laser. When the base of  $Q_1$  is more negative than the base of  $Q_2$ , all

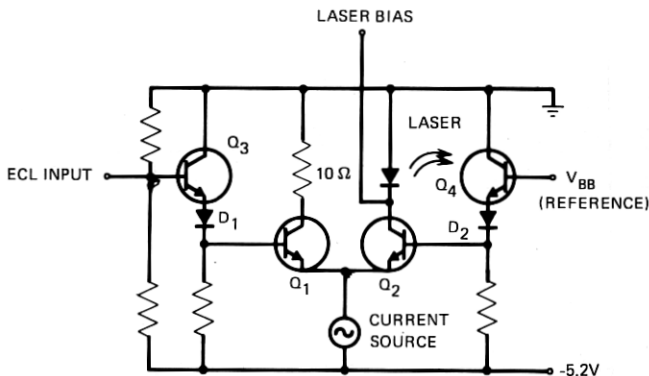


Fig. 2—Emitter-coupled driver circuit.

the drive current is steered through the laser. The selection of one of these conditions is made by an ECL input signal (one =  $-1.8$  V, zero =  $-0.8$  V) applied to the base of  $Q_1$  after level shifting through  $Q_3$  and diode  $D_1$ . The base of  $Q_2$  is fixed at  $-2.6$  V, a voltage midway between the shifted zero and one levels, by a temperature-compensated reference,  $V_{BB}$ .

With an emitter-coupled circuit and with proper choice of input voltage levels, none of the transistors can ever be driven into saturation. This results in fast switching since no stored charge need be removed from a saturated transistor. Another advantage of this driver configuration is its constant-current nature; minimum noise in the form of switching transients is placed on the power bus.

### III. LASER BIAS CIRCUIT

Since the laser is a threshold device and the threshold changes with temperature and aging, the optical power level must be stabilized. This is accomplished using a feedback circuit (Fig. 3) to supply the dc bias  $I_B$  which is adjusted to maintain the peak light output constant relative to a reference. For these transmitters, light from the "back" mirror of the laser crystal is monitored using a p-i-n photodiode while light from the "front" mirror is coupled to the fiber. It was assumed for this development effort that the front and back intensities track each other as a function of temperature and aging, although they need not be equal in magnitude.

In a systems application, it is possible that the input signal may be removed from a channel for an extended period. A simple intensity regulator would tend to raise the bias during such an interval to maintain the average light level expected for ordinary random-data operation. This is not acceptable, since an idle channel would be transmitting half-intensity ones. With a reasonably fast bias circuit, this would occur even during long sequences of zeros in random data, thus generating errors.

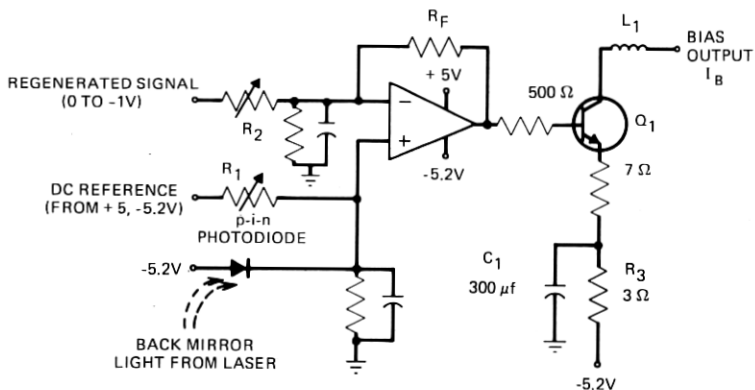


Fig. 3—Bias circuit that provides feedback stabilization of laser output.

To prevent this situation, the input signal pattern is fed to the feedback circuit so that the on, or lasing-light, level is compared with a one and the off, or LED-light, level is compared with a zero. In effect, the dc reference, through resistor  $R_1$  in Fig. 3, sets the bias current at the proper operating point during long sequences of zeros. This bias current, when added to the drive current supplied by the circuit of Fig. 2, results in the desired peak output power. Resistor  $R_2$  then balances the signal reference current against the p-i-n photocurrent for 50 percent duty ratio at 25°C. As the threshold of the laser changes, due either to aging or to changes in ambient temperature, the circuit automatically adjusts  $I_B$  so that the balance between the data reference and the p-i-n photocurrent is restored. The circuit will maintain the LED-light level during long sequences of zeros.

Since the input pattern serves as a precise reference, and also since ECL levels are temperature-dependent, the input signal is thus regenerated to temperature-independent 0-V and -1-V levels before reaching the feedback circuit. This regeneration uses an emitter-coupled driver very similar to Fig. 2 except the collector load resistances of  $Q_1$  and  $Q_2$  are large (500  $\Omega$ ).

The operational amplifier of Fig. 3 sums the three inputs—p-i-n photocurrent, dc reference, and signal pattern reference—and provides an output voltage which results in the proper value of  $I_B$  through the action of transistor  $Q_1$ . This amplifier has unity gain at 800 kHz, permitting small bias corrections to be made in  $\sim 1 \mu\text{s}$ . This correction speed is desirable to prevent amplitude ripple effects resulting from pattern-dependent junction heating, but the circuit is slow enough to ensure stability with a loop gain of approximately 200.

Another function of the feedback circuit is to prevent a transient overshoot of light output from the laser when the power supplies common to both feedback and driver circuits are switched on and off. The scheme adopted here for the turn-on is to let the driver circuit and the

operational amplifier in the feedback circuit reach a steady-state operating condition first while the bias current is slowly increasing. The negative supply voltage to  $Q_1$  in the feedback circuit (Fig. 3) is filtered by  $R_3$  and  $C_1$ , providing an adequately long time constant of  $\sim 1$  ms. Thus by the time the sum of the bias and the drive current reaches threshold, the feedback circuit is ready to limit the laser output to a predetermined magnitude with a minimum overshoot.

#### IV. OPTICAL INTERFACE

The transmission fibers used in the Bell Laboratories lightwave communications experiment had a  $55\text{-}\mu\text{m}$ -diameter,  $\text{GeO}_2$ -doped, graded-index silica core and were clad with silica bringing the glass-fiber outside diameter to  $110\ \mu\text{m}$ . The fiber numerical aperture was approximately 0.23. Nylon jacketing was placed around the fiber for mechanical protection, bringing the diameter up to about  $200\ \mu\text{m}$ . The jacket has no optical function. Typical fibers with these parameters, when coated with DuPont ethylene-vinyl acetate (EVA) and assembled into transmission cables, display an average loss of 6 dB/km at  $825\ \text{nm}$ .<sup>3</sup>

A practical scheme for permanently affixing such a fiber near the stripe geometry laser is to use a single fiber optical jumper cable. This permits initial adjustment of the fiber for maximum coupling, yet still allows the package to be removed from system equipment along with the jumper and its optical connector without disturbing the laser-to-fiber interface. For this purpose a 40-cm jumper, or "pigtail," is assembled. The fiber, which is nylon-jacketed instead of EVA-coated for this application, is placed inside a 2.8-mm O.D. Teflon\* sleeve, which provides additional mechanical protection. A special molded connector<sup>4</sup> is attached at one end, and several millimeters of fiber are left protruding from the Teflon at the other end. A spherical lens is melted on this end of the fiber, the lens raising the coupling from  $\approx 35$  percent without the lens to  $\approx 55$  percent, a gain of 2 dB.<sup>5-7</sup>

During packaging, the Teflon sleeve is attached to the package with a strain-relief bushing, and the free end of the fiber is positioned about  $50\ \mu\text{m}$  in front of the laser (see Fig. 4). A micropositioner is used to position the fiber for maximum coupling (the laser is operated as the light source), and the fiber is then cemented in place. This is a critical step. Coupling efficiencies of 50 to 55 percent are normally attained, but the sensitivity to transverse misalignment (i.e., parallel to plane of laser mirror) is high (see Fig. 5). For example,  $\pm 5\ \mu\text{m}$  in either the  $x$  or the  $y$  direction results in 0.4-dB loss relative to maximum coupling.<sup>8</sup> As shown in Fig. 5, the longitudinal ( $z$ ) direction is much less critical—the  $-1$ -dB point occurs after  $40\ \mu\text{m}$  of motion away from the laser mirror. Once

\* Registered trademark of E. I. DuPont de Nemours and Company.

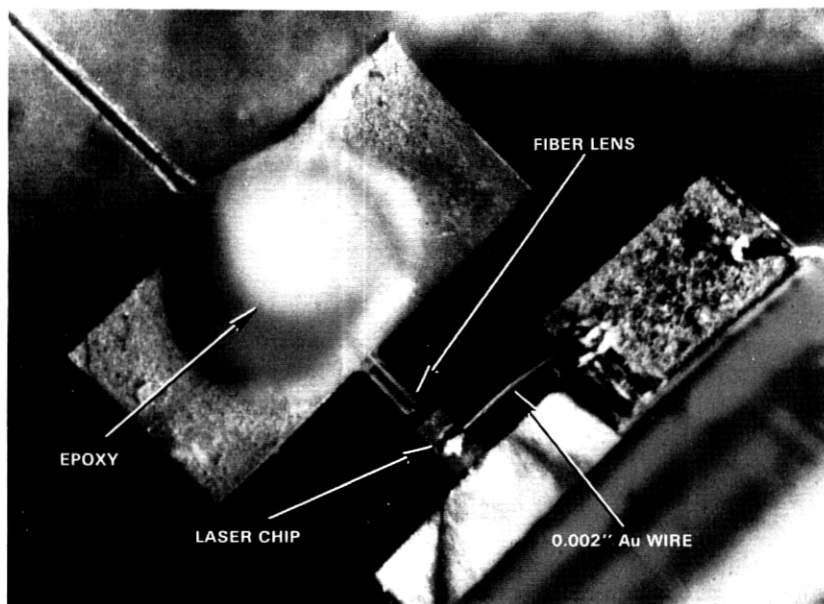


Fig. 4—Photomicrograph (40X) showing wire-bonded laser chip and lensed optical fiber cemented in position (cement is white material over fiber) after alignment.

cemented in place, however, the fibers in these packages have remained stably positioned.

## V. PACKAGING

The two packages forming a complete transmitter subsystem are shown in Fig. 6. The laser and the driver circuit of Fig. 2 are placed in the larger of the two packages ( $5.1 \times 7.0$  cm) along with the fiber pigtail. The second emitter-coupled pair used to regenerate the signal for the feedback circuit is also placed in this package. The feedback circuit, including the series pass transistor for the bias current ( $Q_1$  in Fig. 3), is in the smaller package ( $4.1 \times 6.3$  cm). This separation is done so that the power dissipated by the pass transistor will not interact thermally with the laser. The reasons for packaging the feedback components at all are so that high-reliability beam-lead silicon components can be used and so that all adjustments made during assembly will be sealed off from accidental changes, thus protecting the laser from damaging overdrives.

Components in both packages are bonded to thick-film, hybrid, integrated circuits. The metallization is Pd-Ag and the resistors are made using DuPont 1400 Birox-series paste. It was found that these resistors were stable in the presence of the amine potting epoxy (see the discussion below). Other materials used for resistors might be expected to show severe instability in the presence of amines.<sup>9</sup>

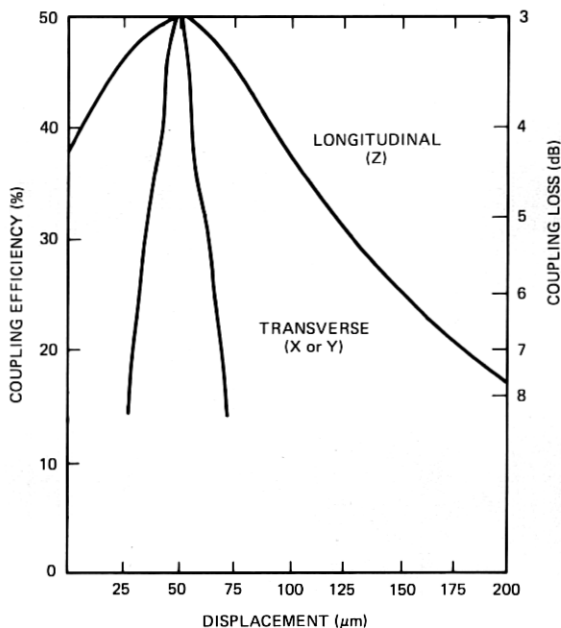


Fig. 5—Sensitivity of power coupled into a 55  $\mu\text{m}$ -core fiber as functions of displacement perpendicular (longitudinal) and parallel (transverse) to plane of laser mirror.

The thick-film circuits, carrying pins for electrical connections, are attached to black-anodized, finned, aluminum heat sinks using silver-filled conductive epoxy. For the laser/driver package (Fig. 7 shows the internal details), a 2.5-cm dia. gold-plated copper header is placed under the thick-film circuit. This header was designed to facilitate heat flow between the laser and the aluminum heat sink. (The laser crystal is indium soldered to a gold-plated, rectangular copper pedestal. The pedestal, in turn, is indium soldered into a slot on the round head.)

As described above, the pigtail sleeve is secured to the driver heat sink. The fiber is positioned using the laser light as a monitor for maximizing the coupling, and the fiber end is cemented near the laser.

For both packages, the circuit is covered with an electromagnetic interference shield. Hysol 4179 potting epoxy is then added, filling out the package (the cavity in Fig. 7) to the outer dimensions of the aluminum heat sink. The p-i-n photodiode used to monitor the back laser mirror for feedback is mounted on a special standoff on the driver circuit (see Fig. 7). Potting materials are kept from obstructing the laser-photodiode optical path by using a plastic shield to create an internal cavity before potting.

One hundred package starts were attempted, resulting in 62 successful completions. Section VI summarizes the measurements made on these subsystems.



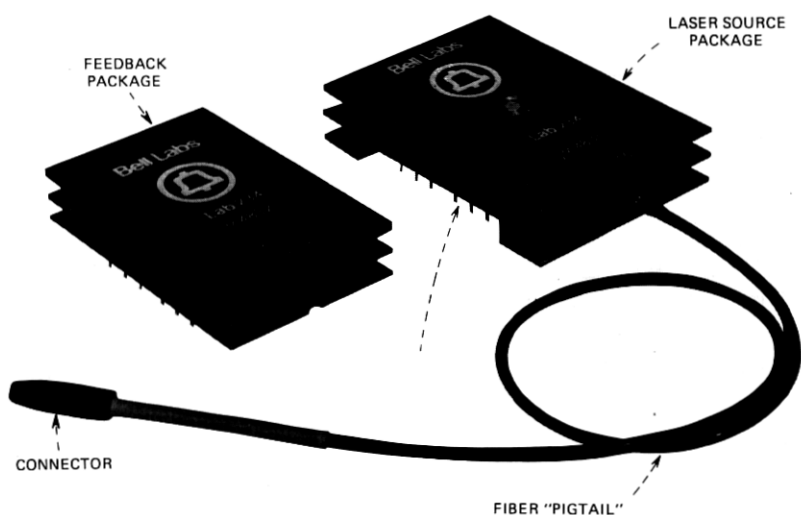


Fig. 6—Transmitter subsystem packages. The laser/driver package is shown on the right and the bias/feedback package on the left.

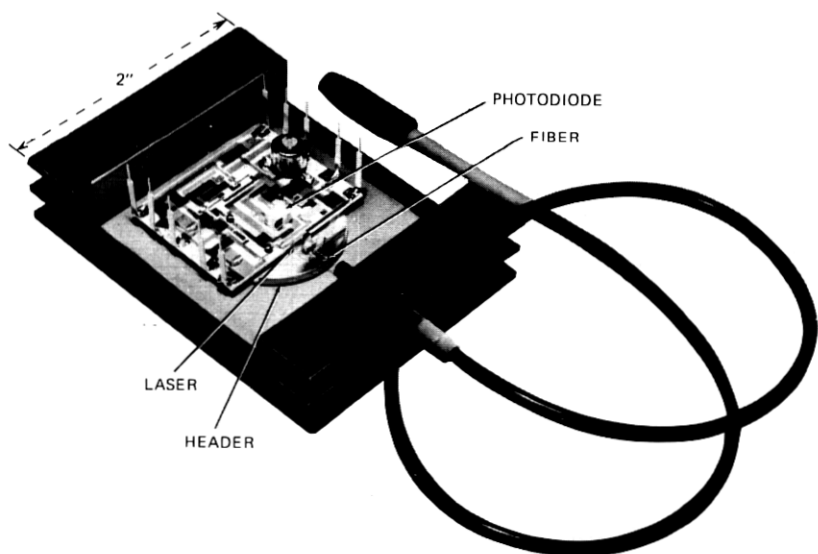


Fig. 7—Laser/driver package shown prior to final potting.

## VI. PERFORMANCE CHARACTERISTICS

Table I lists the design goals for several parameters important to the systems application. These goals were selected for optimum performance of the experimental 44.736-Mb/s link. All goals were met for the completed units.

Table I — Summary of parameter design goals and measured values for 62 packages. Measurements were made at 25°C using a 1023-bit pseudo-random input word

Parameter	Goal	Measured
Average power output @ 25°C	≥0.5 mW	0.63 mW
Average power output @ 50°C	≥0.5 mW	0.63 mW
Amplitude variation (p-p)	≤10%	7%
Propagation delay*	<20 ns	5 ns
Extinction ratio	≥10:1	18:1
Operational temperature range	5–55°C	5–55°C
Power requirement	1.5 W	0.9 W

\* Midpoint of ECL logic transition to midpoint of optical output.

### 6.1 Signal-pattern effects

Figures 8 and 9 show optical-output pulses under various conditions. In Fig. 8, a 500-MHz real-time oscilloscope was used in conjunction with an avalanche photodetector for a resultant rise-time of  $\approx 1.5$  ns. The output was measured at the connector end of the fiber pigtail. Figure 8a shows the optical output for a 0100110100 bit sequence (NRZ at 50 Mb/s). The spiking and relaxation oscillation of light-output pulses were reduced by choosing transistors and components to give a rise-time of  $\approx 2$  ns. (The spiking and oscillations disappear from Fig. 8a because of the slow response of the photodetector used.) Figure 8b shows an "eye" diagram—a superposition of pseudorandom zeros and ones. Such a trace includes the worst and best outputs and, since the pseudorandom sequence is relatively short (1023 bits), the worst-case bits are easily visible (from a duty-cycle point of view). Note that the eye is extremely clean with regard to amplitude ripple. Figure 8c shows the complete 1023-bit word twice using a slow sweep in the upper trace, while the lower trace shows that part of the sequence containing the worst-case pattern—9 zeros followed by 10 ones, at the 6.2-cm mark in the sweep. Notice that the pattern-dependent amplitude ripple is clearly less than 10 percent.

### 6.2 Temperature effects

Figure 9 shows the pulse-shape control supplied by the bias circuit as a function of temperature. For these data, a faster avalanche photodetector was used with a sampling oscilloscope for a resultant rise-time of  $\approx 0.15$  ns. Shorter data pulses lasting 10 ns were also used. The output was measured at the front mirror of the laser. No fiber was in the optical path. Figure 9a shows reasonably clean, constant-width pulses at 0°, 25°, and 45°C. Observe that the relaxation oscillation associated with the leading edge of each pulse is uniformly damped at each temperature. Figure 9b, however, shows the output degradation observed when the feedback loop, adjusted at 25°C, is opened and the temperature changed.

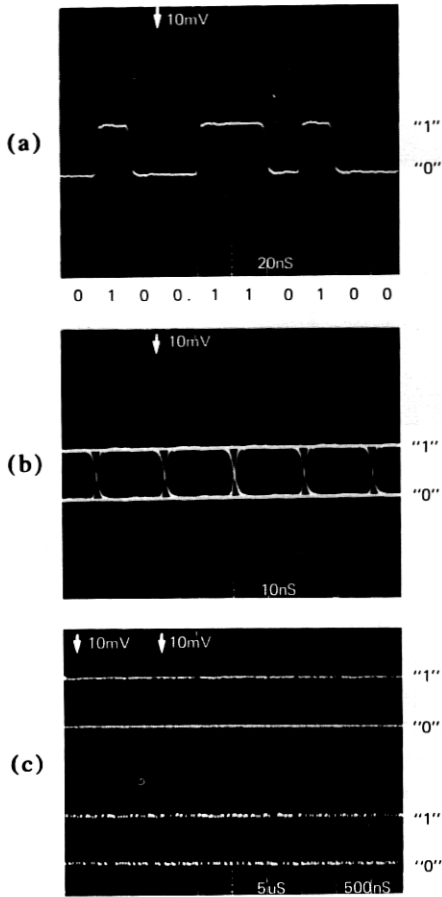


Fig. 8—Oscillographs of optical output as detected using an APD. Horizontal scales ( $t/\text{div}$ ) are shown on each figure. (a) Individual NRZ bits. (b) Eye diagram using a 1023-bit pseudorandom sequence. (c) 1023-bit pseudorandom sequence showing the entire word (upper) and the worst-case sequence (lower), namely, ones after many sequential zeros near the 3, 6, and 9 cm ordinates.

At  $35^{\circ}\text{C}$ , the threshold rises. With the bias still at its  $25^{\circ}\text{C}$  value, the laser is biased too far below threshold, resulting in large relaxation oscillations and increased delay. In addition, the light output is down about 2 dB from its  $25^{\circ}\text{C}$  value. At  $45^{\circ}\text{C}$ , not shown in the figure, no lasing takes place because the sum of bias plus drive is now below threshold. Upon cooling to  $0^{\circ}\text{C}$ , which decreases the threshold, the pulses are excessively wide: biased very near threshold, the delay associated with reaching threshold is absent. The amplitude of the relaxation oscillations is decreased; this would be an advantage if it were not that this occurs only at a particular temperature. Finally, one notices that the light output increases although not as much as expected. This is because the partic-

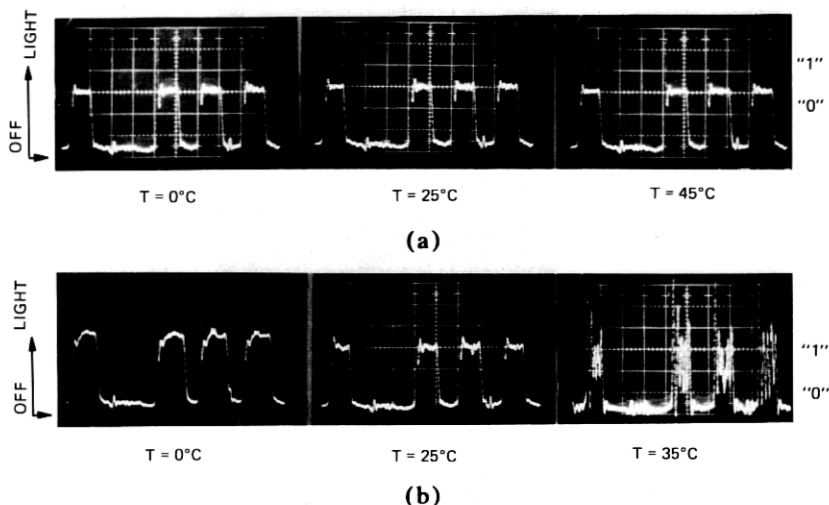


Fig. 9—Light-pulse patterns at various ambient temperatures detected using an APD. Horizontal scales are 10 ns/div. (a) With feedback circuit. (b) With feedback circuit disabled.

ular laser used for these photographs developed a nonlinearity in the operating region of its L-I characteristic at 0°C. Figure 9 clearly shows the stabilization provided by feedback control of the laser bias.

It is instructive to calculate the output-power regulation expected to be provided by the feedback circuit during changes in temperature. From an elementary closed-loop calculation, the light level subject to regulation can be related to temperature-induced threshold shifts as:

$$\frac{dP}{dT} = \frac{\partial P}{\partial I_T} \frac{dI_T}{dT} = - \frac{(1/4)\eta}{1 + A\beta} \frac{dI_T}{dT}, \quad (1)$$

where

$P$  = average light power launched into fiber (mW)

$T$  = temperature (°C)

$I_T$  = laser threshold current (mA)

$\eta$  = laser slope efficiency (mW/mA)

$A$  = transfer gain of amplifier without feedback

$\beta$  = reverse transmission factor.

The last factor  $\beta$  is a function of the p-i-n diode's quantum efficiency, the slope efficiency of the laser diode, and the coupling between the laser and the p-i-n diode. Typical values are:

$P = 0.63$  mW

$I_T = 100$  mA ( $T = 25^\circ\text{C}$ )

$\eta = 0.2$  mW/mA (for each mirror)

$$A = 23000$$

$$\beta = 0.01$$

The factor of 1/4 in the numerator of (1) adjusts laser peak power for a 50-percent duty cycle (for random signals) and for the 50-percent coupling efficiency to the fiber. Since the threshold of these lasers shifts approximately +1 mA/°C, which is  $dI_T/dT$ , (1) gives

$$\frac{dP}{dT} = -0.2 \mu W/^\circ C. \quad (2)$$

Experimentally, a typical package showed a  $\leq 1$  percent power decrease as the package temperature was raised from 25°C to 50°C. For the data used above, this gives  $dP/dT \approx -0.25 \mu W/^\circ C$ , in very good agreement with the prediction in (2).

### 6.3 Aging effects

Approximately half the 62 completed units were used in the Bell Laboratories experiment, while the others were aged under normal operating conditions at 25° or 50°C. The principal aging characteristic of these lasers is a gradual increase of threshold current with time. Thus at either temperature, the closed-loop bias circuit should hold the output power quite constant with time until the circuit can no longer supply adequate current for a greatly shifted threshold. The circuit described here limits at about 225 mA. When the threshold, initially  $\sim 100$  mA, reaches this value, the output power will begin to decrease as the laser continues to age. For both the 25° and 50°C packages, however, while some package outputs did remain constant with time, others showed increasing or decreasing power trends. Approximately as many packages showed increasing power as showed decreasing power.

A careful analysis of these packages showed that the feedback control circuitry was performing properly but that the front and back laser mirrors mistracked slightly.<sup>10</sup> Therefore, while the feedback circuit was maintaining constant power at the back mirror, the power launched into the fiber from the front mirror was not precisely regulated.

For power stability with aging, (1) can again be used if  $dI_T/dT$  is replaced by  $dI_T/dt$ , the value of, at most, +1 mA/1000 h.<sup>11</sup> Thus

$$\frac{dP}{dt} \leq -0.2 \mu W/kh.$$

Due to the front-to-back mistracking, however, the output of our units varied from less than 10 to as much as 100 times more than this prediction, as well as changing in either direction, although the back-mirror power was maintained constant to within the resolution of our apparatus ( $\pm 3 \mu W$ ). For future transmitter designs, the power actually launched into the fiber should be monitored for feedback-control purposes unless lasers, at that time, demonstrate better front-to-back tracing.

## VII. SUMMARY AND CONCLUSIONS

An optical communications source has been designed for use at 44.736 Mb/s. Sixty-two such transmitters were completed, meeting the design goals and clearly demonstrating the viability of using GaAlAs injection lasers for stable optical sources in lightwave communications. It is concluded that feedback control of laser bias is a practical solution for regulating output power. It was found, however, that unless the front and back mirrors of GaAlAs lasers can be made to track each other linearly, the light power actually launched into the transmission fiber should be monitored to assure maximum power stability.

## VIII. ACKNOWLEDGMENTS

We thank B. C. DeLoach, R. W. Dixon, R. L. Hartman, and B. Schwartz for supplying the GaAlAs lasers used for this work, G. Moy for his careful measurements on all these devices, and D. R. Mackenzie for developing the soldering technique for mounting the laser pedestals. Thanks also go to D. D. Sell for his comments and suggestions concerning the feedback scheme, to P. K. Runge for supplying connectors for the pigtailed, to the Thick-Film Technology Group at the Allentown laboratory of Bell Laboratories for supplying the thick-film circuits, and to W. W. Benson for the data used in Fig. 5. We thank M. DiDomenico for his guidance and technical suggestions that contributed substantially to the project. Finally, we especially thank E. E. Becker, D. P. Hansen, R. Pawelek and J. R. Potopowicz for their expert assistance in package assembly, and M. A. Karr for the package design and assistance with assembly.

## REFERENCES

1. T. L. Maione and D. D. Sell, "Experimental Fiber-Optic Transmission System for Interoffice Trunks," IEEE Trans. Commun., to be published.
2. S. D. Personick, "Receiver Design for Digital Fiber Optic Communications Systems, II," B.S.T.J., 52, No. 6 (July-August 1973), pp. 875-86.
3. M. I. Schwartz, R. A. Kempf, and W. B. Gardner, "Design and Characterization of an Exploratory Fiber-Optic Cable," Second European Conf. on Optical Fiber Communication, Paris 1976, paper X.2.
4. J. S. Cook and P. K. Runge, "An Exploratory Fiberguide Interconnection System," Second European Conf. on Optical Fiber Communication, Paris 1976, paper VIII.3.
5. D. Kato, "Light Coupling from a Stripe-Geometry GaAs Diode Laser into an Optical Fiber with Spherical End," J. Appl. Phys., 44 (1973), pp. 2756-2758.
6. L. G. Cohen and M. V. Schneider, "Microlenses for Coupling Junction Lasers to Optical Fibers," Appl. Opt., 13 (1974), pp. 89-94.
7. C. A. Brackett, "On the Efficiency of Coupling Light from Stripe-Geometry GaAs Lasers into Multimode Optical Fibers," J. Appl. Phys., 45 (1974), pp. 2636-2637.
8. W. W. Benson, private communication.
9. K. Asama, Y. Nishimura, and H. Sasaki, "Study on the Thick-Film Resistance Abrupt Change by Resin Packaging," Proc. 1969 Hybrid Microelectronics Symposium, pp. 51-62.
10. T. L. Paoli, "Nonlinearities in the Emission Characteristics of Stripe-Geometry (Al-Ga)As Double-Heterostructure Junction Lasers," IEEE J. Quantum Electron., QE-12, No. 12 (Dec. 1976), pp. 770-776.
11. R. L. Hartman, private communication.